European Journal of Medicinal Chemistry 47 (2012) 412–423

Contents lists available at SciVerse ScienceDirect

European Journal of Medicinal Chemistry

journal homepage: http://www.elsevier.com/locate/ejmech

Original article

First chemical feature-based pharmacophore modeling of potent retinoidal retinoic acid metabolism blocking agents (RAMBAs): Identification of novel RAMBA scaffolds

Puranik Purushottamachar [a,c], Jyoti B. Patel [c,1], Lalji K. Gediya [a,c], Omoshile O. Clement [d,2], Vincent C.O. Njar [a,b,c,*]

[a] Department of Pharmaceutical Sciences, Jefferson School of Pharmacy, Thomas Jefferson University, 130 South 9th Street, Philadelphia, PA 19107, USA
[b] Kimmel Cancer Center, Thomas Jefferson University, 233 South 10th Street, Philadelphia, PA 19107, USA
[c] Department of Pharmacology and Experimental Therapeutics, University of Maryland School of Medicine, 685 West Baltimore Street, Baltimore, MD 21201, USA
[d] Accelrys Inc., 10188 Telesis Court, Ste 100, San Diego, CA 92121, USA

ARTICLE INFO

Article history:
Received 9 September 2011
Received in revised form
31 October 2011
Accepted 3 November 2011
Available online 17 November 2011

Keywords:
Common feature-based pharmacophore hypotheses
HipHop
Retinoic acid metabolism blocking agents (RAMBAs)
Docking
Quantitative structure–activity relationships
Anti-cancer agents

ABSTRACT

The first three-dimensional (3D) pharmacophore model was developed for potent retinoidal retinoic acid metabolism blocking agents (RAMBAs) with IC_{50} values ranging from 0.0009 to 5.84 nM. The seven common chemical features in these RAMBAs as deduced by the Catalyst/HipHop program include five hydrophobic groups (hydrophobes), and two hydrogen bond acceptors. Using the pharmacophore model as a 3D search query against NCI and Maybridge conformational Catalyst formatted databases; we retrieved several compounds with different structures (scaffolds) as hits. Twenty-one retrieved hits were tested for RAMBA activity at 100 nM concentration. The most potent of these compounds, NCI10308597 and HTS01914 showed inhibitory potencies less (54.7% and 53.2%, respectively, at 100 nM) than those of our best previously reported RAMBAs VN/12-1 and VN/14-1 (90% and 86%, respectively, at 100 nM). Docking studies using a CYP26A1 homology model revealed that our most potent RAMBAs showed similar binding to the one observed for a series of RAMBAs reported previously by others. Our data shows the potential of our pharmacophore model in identifying structurally diverse and potent RAMBAs. Further refinement of the model and searches of other robust databases is currently in progress with a view to identifying and optimizing new leads.

1. Introduction

During the last 30 years, research into cancer treatment has focused mainly on the use and development of cytotoxic agents. However, despite significant progress in the chemotherapy of some malignancies such as testicular carcinoma and lymphomas, the prognosis of patients with the most common invasive and metastatic tumors remains poor [1]. There is a clear need for new treatment approaches which ultimately may be met by novel ideas coming from recent advances in understanding the underlying biology of cancer. Cancer cells show various degrees of differentiation, and there normally is an inverse relation between the degree of cell differentiation and the clinical aggressiveness of a cancer [2].

However, certain chemicals (differentiating agents) are capable of redirecting the cells to the normal phenotype of morphologic maturation and loss of proliferative capacity. Consequently, differentiating agents may reverse or suppress evolving lesions to prevent cancer invasion [1,3–5]. Differentiating agents thus offer an attractive potential alternative to conventional cytotoxic agents. One group, the retinoids, constitute a class of chemical compounds, including vitamin A and its synthetic and naturally occurring analogs, that have been the subject of extensive scientific and clinical investigations [3,6,7].

Abbreviations: 3D, three-dimensional; 3D-QSAR, three-dimensional quantitative structure–activity relationships; ARDAs, androgen receptor down-regulating agents; ATRA, all-*trans*-retinoic acid; GH, Güner–Henry; Hypos, hypotheses; MOE, molecular operating environment; RAMBAs, retinoic acid metabolism blocking agents; RAR, retinoic acid receptor.

* Corresponding author. Department of Pharmaceutical Sciences, Jefferson School of Pharmacy, Thomas Jefferson University, 130 South 9th Street, Philadelphia, PA 19107, USA. Tel.: +1 215 853 7468; fax: +1 215 503 9052.
E-mail address: vincent.njar@jefferson.edu (V.C.O. Njar).
[1] Present address: Division of Bioequivalence and GLP compliance Office of Scientific Investigations/Office of Compliance, CDER FDA, 10903 New Hampshire Avenue, Silver Spring, MD 20993, USA.
[2] Present address: Biomatrica, Inc., 5627 Oberlin Court, Ste 120, San Diego, CA 92121, USA.

0223-5234/$ – see front matter © 2011 Elsevier Masson SAS. All rights reserved.
doi:10.1016/j.ejmech.2011.11.010

Retinoids, natural and synthetic analogs of all-*tans*-retinoic acid [8], play a key role in many biological functions, including induction of cellular proliferation, differentiation, and apoptosis, as well as developmental changes [9]. ATRA exerts its activity through binding with transcription-regulatory factors, known as the retinoic acid receptors (RAR), of which there are three subtypes; RARα, RARβ and RARγ. ATRA and several synthetic retinoids are currently used in cancer differentiation therapy, cancer chemoprevention, and treatment of dermatological diseases [10,11]. One of the most impressive effects of ATRA is on acute promyleocytic leukemia (APL). Treatment of many APL patients with high doses of ATRA has resulted in complete remission [12]. However, the clinical use of ATRA in the treatment of cancers is significantly hampered by the prompt emergence of resistance, which is believed to be caused at least in part by increased ATRA metabolism.

One of the strategies for preventing *in vivo* catabolism of ATRA is to inhibit the P450 enzyme(s) responsible for this process. Inhibitors of ATRA metabolism (also referred to as retinoic acid metabolism blocking agents (RAMBAs)) may prove useful for the chemoprevention and/or treatment of various kinds of cancer [13,14], and also for the treatment of various kinds of dermatological diseases [15,16]. The major pathway of metabolic deactivation of ATRA starts with hydroxylation at C-4 to form 4-hydroxy-ATRA, which is then oxidized into 4-oxo-ATRA. 4-Oxo-ATRA is further transformed into more polar metabolites [17] . The first and the rate limiting step in this process is catalyzed by a cytochrome P450 dependent 4-hydroxylase enzyme. Although several human CYPs have been shown to be capable of converting ATRA to more polar metabolites, their specificity for ATRA is generally moderate. Recently, while CYP2C8 was reported to be a major contributor to ATRA 4-hydroxylation in the human liver [18,19], Marill *et al.* [20] identified CYP3A7 to be the most active enzyme responsible for ATRA metabolism. In addition, CYP26 has been identified as the most dedicated ATRA 4-hydroxylase [21–25]. CYP26 recognizes only ATRA as its substrate, and its expression and/or activity can be induced by ATRA both *in vitro* and *in vivo*. In adult humans, CYP26 is expressed in several tissues, mainly in liver, adrenals, heart, and hypothalamus [26]. Perhaps of more significance of this work was the realization that a variety of human cancer cells and tumors have been shown to possess ATRA 4-hydroxylase activity [27–34]. Irrespective of the CYP isoenzyme(s) involved, increased metabolism of ATRA could generate a condition of retinoid [8] deficiency, which is implicated in cancers and dermatological diseases. Thus, agents that can prolong and intensify the action of endogenous ATRA by inhibiting ATRA metabolizing enzymes can be potentially used as clinical agents in the treatment of the aforementioned diseases.

Several categories of non-retinoidal RAMBAs have been reported in literature [13,14,16,35–37], but only a few retinoidal RAMBAs, developed by our group, are known [14,38,39]. Our RAMBAs are considered to be atypical, because in addition to being potent inhibitors of ATRA metabolism (CYP26 inhibitors that are able to enhance the antiproliferative action of ATRA), they also possess intrinsic potent cancer antiproliferative activities [14,38–45].

The rational design of RAMBAs with *novel scaffolds* would be greatly helped by knowledge of the three-dimensional structure of the enzyme (CYP26). Although there is currently no crystal structure information on known RAMBAs bound to CYP26, recent studies on a homology model of human retinoic acid metabolizing enzyme (CYP26A1) has identified putative structurally and functionally important residues of the enzyme's active/binding sites [46].

Because there is no molecular pharmacophore modeling studies on RAMBAs and also because of the exceptional potencies of our retinoidal RAMBAs, we considered it a worthy research endeavor to analyze our potent RAMBAs by three-dimensional quantitative structure–activity relationship (3D-QSAR) software program, Catalyst [47]. The hypotheses generation methods (HipHop and HypoGen) of the Catalyst software is one of the methods for rational drug design, which has been successfully applied in drug discovery research [48–53] (for more comprehensive references lists see http://www.accelrys.com/references/rdd_pub.html).

Previously, we successfully employed pharmacophore perception strategy in the discovery of novel human CYP17 inhibitors [48] and androgen receptor down-regulating agents (ARDAs) [49]. The Catalyst program can be used to probe how ligands interact with a receptor/enzyme by evaluating chemical feature common to a set of active ligands (HipHop) [54] or by elucidating the correlation between activity and chemical binding features (HypoGen) [55]. The hypotheses generated may be used to estimate the biological activity of proposed target, allowing a rank ordering of synthetic priorities. In addition, the hypotheses generated may be used as three-dimensional queries to search databases of proprietary and/or commercially available compounds. These three-dimensional searches could identify novel chemical scaffold that might exhibit potent inhibition of the target enzyme. The large number of successful applications of 3D pharmacophore-base searching in medicinal chemistry clearly demonstrates its utility in the modern drug discovery paradigm [48–53].

The HipHop algorithm finds common features pharmacophore models among a set of highly active compounds thus carrying out a 'qualitative model' without the use of activity data, which represents the essential 3D arrangement of functional groups common to a set of molecules for interacting with specific biological targets. As there is a high structural homology among the derivatives combined with narrow activity range, the HipHop method was used in this study. We believe that the common feature pharmacophore developed from the potent RAMBAs evaluated under the same assay condition could lead to the discovery of potent RAMBAs with novel scaffolds.

In this report, we present the development of the first pharmacophore models of RAMBAs using the Catalyst/HipHop module. Following evaluation of the generated models for selection of best hypo, we used the best hypotheses for database searching followed by pharmacological evaluation of hit molecules to identify new RAMBAs with non-retinoidal scaffolds. Furthermore, we report docking results of some selective leads and hit molecules with CYP26A1 homology model.

2. Results and discussion

2.1. Structures and biological activities of training set compounds

Table 1 shows the structure of five compounds and their IC_{50} values for CYP26 (hamster liver microsomal assay) inhibition determined in our laboratory under the same assay conditions [39]. The range of CYP26 inhibition activity exhibited by these compounds was 0.009–5.84 nM. This range of inhibition activity (3 log units) and small set of molecules was not large enough to allow us to generate meaningful activity-based (predictive) pharmacophore models using Catalyst/HypoGen technology. However, on the assumption that the most active compounds bind in a similar fashion at the enzyme's active site, we employed the Catalyst/HipHop approach to evaluate the common feature required for binding and the hypothetical geometries adopted by these ligands in their most active forms. Thus, a training set consisting of five of the most active RAMBA inhibitors (**3**–**7**; see Table 1) was submitted for pharmacophore model generation based on common chemical features.

Table 1
Chemical structures of five training set molecules[a] used to generate the common feature (HipHop) pharmacophore model.

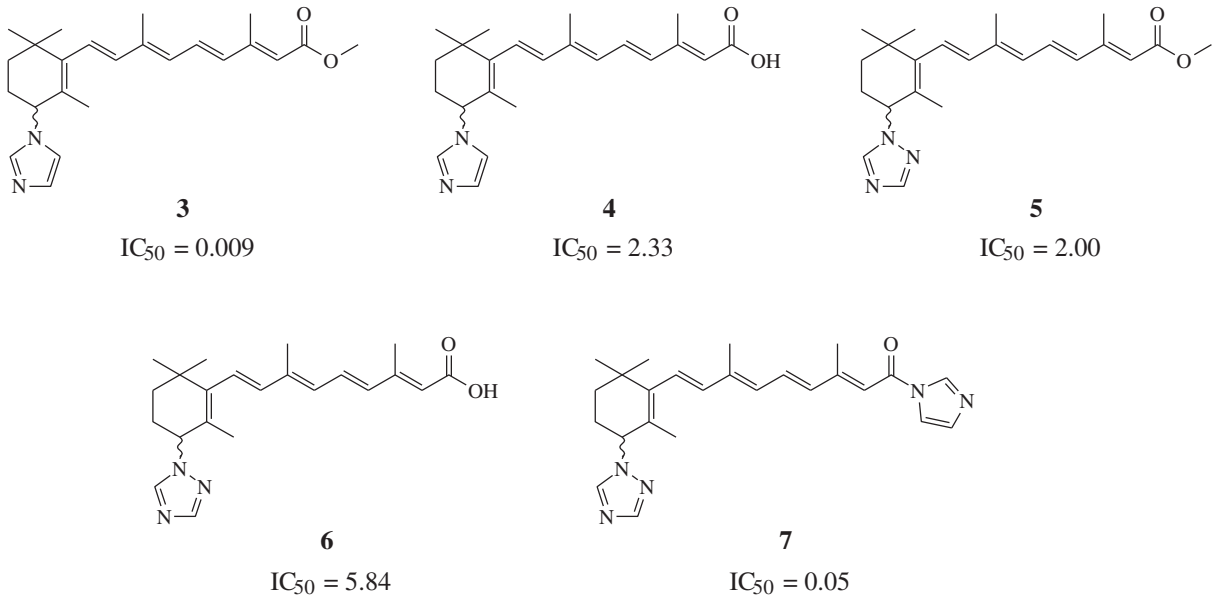

[a] Detailed information of synthesis and biological data is reported elsewhere [39,43]. *In vitro* inhibition of ATRA metabolism by hamster liver assay (IC_{50} values in nM).

2.2. Pharmacophore modeling

2.2.1. 3D pharmacophore generation

In the model generation methodology, the highest weighting was assigned to the most active compound in the training set (compound **3**; IC_{50} 0.009 nM), this was achieved by putting 2 (which ensures that all of the chemical features in the compound will be considered in building hypotheses space) and 0 (which forces mapping of all features of compound) in principle and maximum omitting features columns, respectively, for the most active compound, and 1 (ensures that at least one mapping for each of generated hypotheses will be found), 1 (all but one feature must map) in principle and maximum omitting feature column respectively for all other compounds (for a detailed description of these input parameters see the Catalyst 4.10 Tutorial: http://www.accelrys.com/doc/life/catalyst410/tutorials/cat410_tutsTOC.html). All other parameters were kept at default.

The ten hypotheses (hypos) generated had scores from 86.87 to 90.62 (Table 2). This small range of ranking score suggests that the features are spatially arranged in a similar fashion in all 10 models.

Table 2
Summary of hypotheses run.

Hypo	Feature[a]	Rank	Direct it mask	Partial hit mask
1	HHHHHAA	90.62	11111	00000
2	RHHHHHA	90.32	11111	00000
3	HHHHHAA	90.16	11111	00000
4	RHHHHHA	89.57	11111	00000
5	HHHHHAA	89.38	11111	00000
6	HHHHHAA	88.66	11111	00000
7	RHHHHHA	87.91	11111	00000
8	HHHHHAA	87.88	11111	00000
9	RHHHHHA	87.55	11111	00000
10	RHHHHHA	86.87	11111	00000

Direct hit mask indicates [1] or (0) not a training set molecule mapped every feature. Partial hit mask indicates whether [1] or (0) not a molecule mapped all but one feature.

[a] H; hydrophobic, A; hydrogen bond acceptor (HBA) and R; ring aromatic.

To determine the similarity between the ten hypotheses, a hierarchical cluster analysis was performed. The results of the cluster analysis indicate that hypos 1 and 6, 2 and 4, 3 and 8, and 7 and 10 belong to the same cluster, whereas hypos 5 and 9 are slightly different. All ten hypotheses contain seven features, of which five hydrophobic (H) features are common for all. Five hypotheses contain two hydrogen bond acceptors (HBAs) and the remaining five hypotheses contain one HBA and one ring aromatic (R) feature (Table 2). The cyclohexene ring and aliphatic polyene chain in the molecules are recognized as hydrophobic, and the acid and ester groups on the aliphatic polyene chain-end are recognized as hydrogen bond acceptors in all hypotheses. However, the heterocyclic ring on cyclohexene ring in all molecules is recognized as hydrogen bond acceptor in hypotheses 1, 3, 5, 6 and 8 and as ring aromatic in hypotheses 2, 4, 7, 9 and 10.

Selection of the best hypotheses was performed using the Güner–Henry (GH) scoring method [56] as well as knowledge of the 3D structure of the ligand–enzyme interactions. GH scoring methodology has been successfully applied to quantification of model selectivity and coverage of activity space from database mining [57] and to the evaluation of the effectiveness of similarity search in databases containing both structural and biological activity data [58]. It is well known that all CYP enzymes contain heme as a prosthetic group, which is essential for their catalytic action. Functional groups such as hydrogen bond acceptors are known to act as the sixth ligating atom interaction with Fe(II) of heme in most CYP enzyme inhibitors. Considering the robust application of both the GH method and 3D structural information of ligand–enzyme interactions, we adapted these two criteria for selection of best hypo as described below.

The GH analysis was done by computing the following variables: (a) the percent yield (%*Y*), which is a measure of the selectivity of the model, (b) the percent active (%*A*), which represents the coverage of activity space by the model, (c) the enrichment factor (*E*), and (d) the GH score. These variables (see Chart 2) are determined using information derived from the total number of compounds in the drug database (*D*), the number of actives in the

Table 3
Pharmacophore model evaluation based on the Güner–Henry scoring method [63].

Database	Features	H_t	H_a	%A	%Y	E	GH
		1005[a]	5	100.0	0.50	1.00	0.00
Hypo 1	HHHHHAA	12	5	100.0	41.67	83.8	0.559
Hypo 2	RHHHHHA	5	5	100.0	100.00	201.0	1.000
Hypo 3	HHHHHAA	18	4	80.0	22.22	44.7	0.362
Hypo 4	RHHHHHA	6	5	100.0	83.33	167.5	0.874
Hypo 5	HHHHHAA	18	5	100.0	27.78	55.8	0.452
Hypo 6	HHHHHAA	15	5	100.0	33.33	67.0	0.495
Hypo 7	RHHHHHA	6	5	100.0	83.33	167.5	0.874
Hypo 8	HHHHHAA	18	5	100.0	27.78	55.8	0.452
Hypo 9	RHHHHHA	7	5	100.0	71.43	143.6	0.784
Hypo 10	RHHHHHA	6	5	100.0	83.33	167.5	0.874

[a] Total number of compounds in Catalyst modified WDI2003 is 1005, and the total number of RAMBAs in this modified database (*A*) is 5. H_t = no. of hits retrieved; H_a = no. of actives in hit list; %*A* = ratio of actives retrieved in hit list; %*Y* = fraction of hits relative to size of database (hit rate of selectivity); *E* = enrichment of active bin by model relative to random screening; GH = Güner–Henry score.

Table 4
Best fit values of five best hypotheses which retained after GH analysis.

Compd	Activity IC_{50} nM	Confon[c]	Fit value[d]				
			Hypo 2	Hypo 4	Hypo 7	Hypo 9	Hypo 10
3	0.009[a]	59	7.0	7.0	7.0	7.0	7.0
4	2.33[a]	47	5.4	4.8	5.8	5.8	5.8
5	2.0[a]	69	6.4	5.5	5.3	5.3	5.3
6	5.84[a]	55	5.4	5.2	6.1	6.3	6.4
7	0.05[a]	35	4.9	4.7	5.5	5.5	5.3
2	14.4[b]	249	6.7	–	–	–	–

[a] *In vitro* inhibition of ATRA metabolism by hamster liver assay [43].
[b] A biochemical assay was performed using microsomal preparations from T47D cells induced to express CYP26 [59].
[c] A diverse set of conformations for all molecules was generated by using 'Best conformer generation' option with 20 kcal/mol energy cutoff [61].
[d] Compare fit analysis of all compounds with maximum omitting feature value as 1.

database (*A*), the number of actives retrieved by the model (H_a), and the total number of hits retrieved by the model (H_t).

2.2.2. Pharmacophore selection and validation

A text-based query using mechanism of action (MOA) in the search field was used to search for RAMBAs in the modified Derwent World Drug Index (WDI2003). Initially a Catalyst formatted database was created by combining five molecules of the training set and 1000 molecules from the WDI2003 database with molecular weight range 360–420 (cut of MW range similar to the training set RAMBA molecules). This Catalyst formatted database of 1005 compounds was used to screen all ten hypotheses in order to evaluate the parameters – %*A*, %*Y*, *E* and GH score. The search

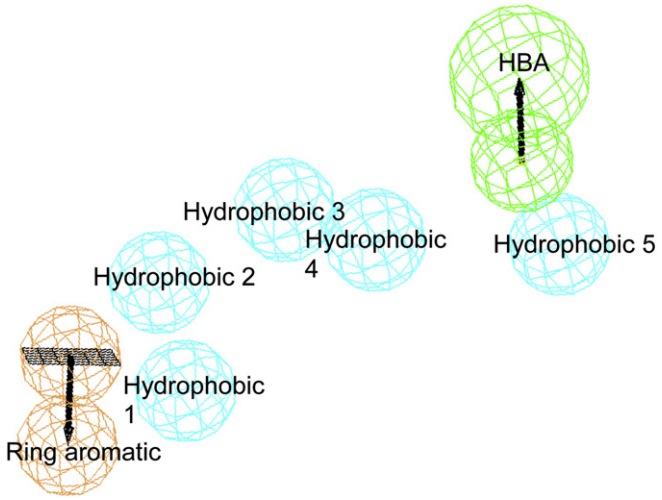

Fig. 2. Common feature-based (Catalyst/HipHop) pharmacophore model of all-*trans*-retinoic acid based RAMBA inhibitors selected on the results of GH analysis (hypo 2). The model contains seven features: five hydrophobic (cyan), one hydrogen bond acceptors (green) and one ring aromatic (red). (For interpretation of the references to color in this figure legend, the reader is referred to the web version of this article.)

results are shown in Table 3. On the basis of the GH analysis results, hypotheses #2, 4, 7, 9 and 10 with best GH score (0.784–1.0) and Enrichment factor (>140) were selected for further analysis. Additional pruning of these five hypotheses was based on the fit score of hypos with training set molecules (Table 4). Ideally, the best hypo should yield a fit score range that mimic the activity trend and the magnitude difference in activities. From the results of fit scores in Table 4, it is difficult to select the overall best hypo based on this analysis. However, hypos #2 and 4 show somewhat better fit scores than the others. These two hypos yield fit scores that correlate with activity trend for three out of the five RAMBAs in the training set; both hypos (#2 and #4) have similar functional features and are in the same cluster. Of the two hypos, #2 provided the overall better alignment with the RAMBA training set compounds (Fig. 1a and b), than hypo #4. In addition, hypo #2 has the highest enrichment (201) and a perfect GH score, and hence was selected as the best hypothesis for the class of these RAMBA compounds.

This pharmacophore model contains seven chemical features: five hydrophobic (HYD; cyan), one hydrogen bond acceptor (HBA; green) and one ring aromatic (RA; brick red) (Fig. 2). The HBA maps the carbonyl oxygen of the carboxylic group on the aliphatic chain, while the heterocyclic aromatic ring attached to the cyclohexene ring maps the ring aromatic (RA). Hypo #2 was further evaluated against a known drug candidate from OSI Pharmaceutical –

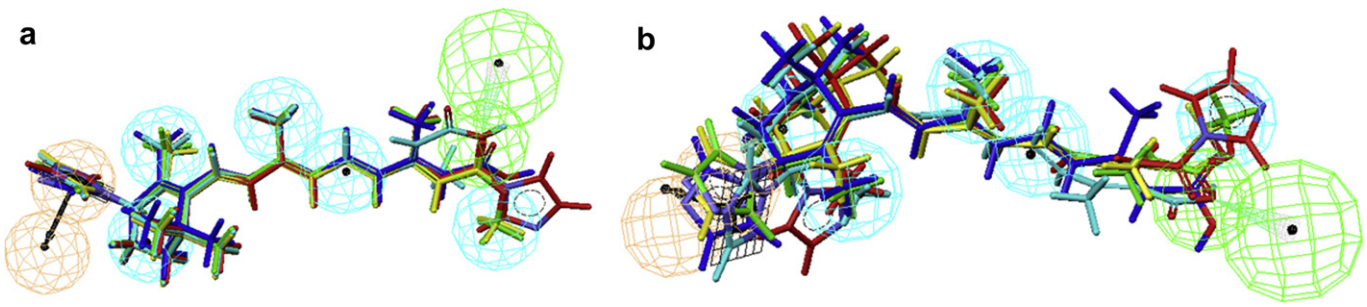

Fig. 1. Alignment of common feature pharmacophore models hypo 2 (**1a**) and hypo 4 (**1b**) with training set molecules.

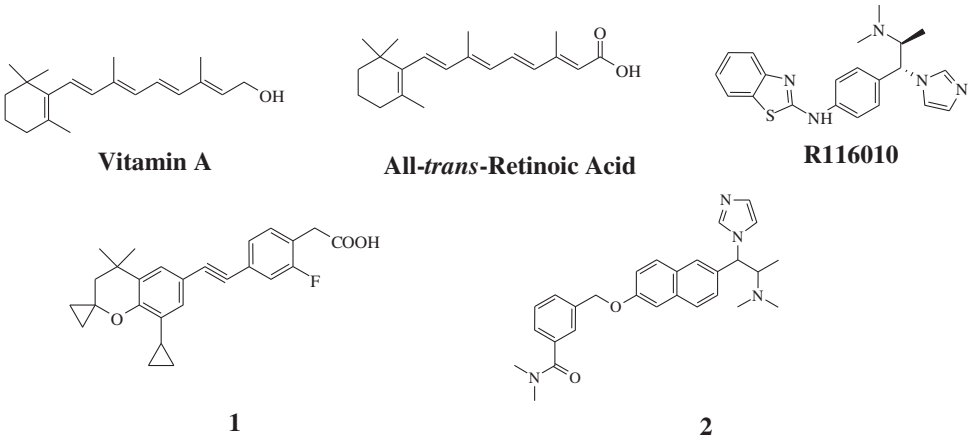

Chart 1. Structures of retinoid, all-*trans*-retinoic acid and three potent ATRA 4-hydroxylase inhibitors.

$$\%A = \frac{H_a}{A} \times 100$$

$$\%Y = \frac{H_a}{H_t} \times 100$$

$$E = \frac{H_a/H_t}{A/D}$$

$$GH = \frac{H_a(3A + H_t)}{4(H_tA)} \quad \left(1 - \frac{H_t - Ha}{D - A}\right)$$

Chart 2. Metrics for analyzing hit lists in pharmacophore-based modeling [56]. [a] H_t = no. of hits retrieved; H_a = no. of actives in hit list; $\%A$ = ratio of actives retrieved in hit list; $\%Y$ = fractions of hits relative to size of database (hit rate or selectivity); E = enrichment of active bin by model relative to random screening; GH = Güner–Henry score.

compound **2** in Chart 1, which is a potent RAMBA [59]. Thus, a diverse set of conformers for compound **2** (249 conformers) was generated by a similar protocol as described for the RAMBA training set molecules used in generating the hypotheses. Thereafter, compound **2** was aligned with hypo #2 to generate an excellent align/fit score of 6.7 out of 7 features (Fig. 3). From this data, we conclude that the selection of hypo #2 is reasonable and provides confidence for the utility of the chemical feature-based pharmacophore model to retrieve structurally diverse compounds with desired biological activity (For interpretation of the references to color in this paragraph, the reader is referred to the web version of this article.).

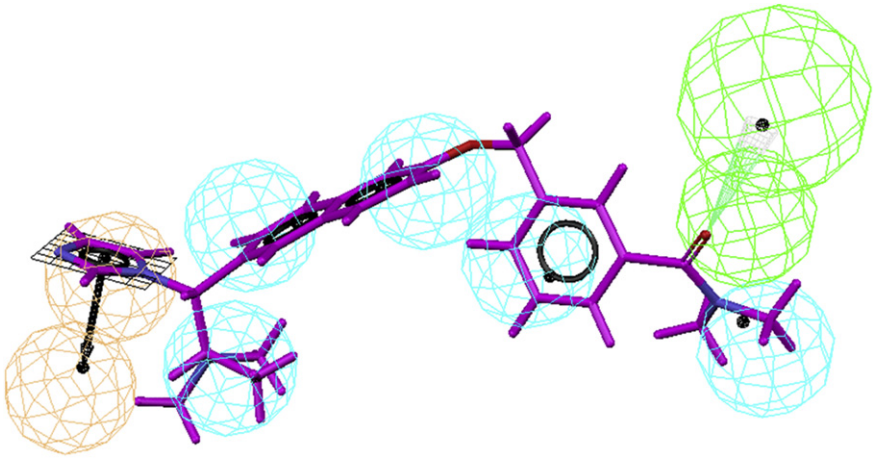

Fig. 3. Alignment of compound **2** with hypo 2.

For the selection of best hypo on the basis of knowledge of ligand–enzyme interaction we selected five hypos (#1, 3, 5, 6 and 8) with two HBA functionalities. Of these five hypos, three (hypos #1, 3 and 5) were retained for further analysis as determined by the ranking of the HipHop models and by elimination of redundancies based on hierarchical clustering of the five hypotheses. Further pruning of the remaining three hypotheses was based on the criteria that of all the top ranking hypotheses, the hypotheses which maps all important features of the active compounds and if possible to some extent show correlation between best fit values, conformational energies and actual activities of the training set. Hypo 3 was selected as best hypotheses as it shows good alignment with training set molecules (Fig. 4a) and correlation in fit values in comparison with hypos 1 and 5 (Table 5). This pharmacophore model contained seven chemical features: five hydrophobes (cyan) and two hydrogen bond acceptor (green) chemical features (Fig. 4b). The HBAs map the carbonyl oxygen of carboxylic group on aliphatic chain and the N atom of the heterocyclic ring attached to the cyclohexene ring. Hypo #3 was further evaluated against OSI pharmaceutical's compound **2** (Fig. 4c) as described above for hypo #2. This molecule also fits hypo #3 with a fit score of 5.36.

To identify the best representative pharmacophore hypothesis among the two selected hypos (hypo #2 and hypo #3) obtained from GH analysis and knowledge of ligand–enzyme interaction respectively, we also evaluated the quality (biological activity profiles) of the compounds retrieved from the NCI and Maybridge databases by both hypos #2 and 3.

Table 5
Best fit values of three hypotheses which retained after hierarchical clustering.

Compd	Activity	Fit value		
		Hypo 1	Hypo 3	Hypo 5
3	0.009	6.99	6.99	6.98
4	2.33	5.91	5.94	5.94
5	2.0	6.85	6.65	6.72
6	5.84	6.85	5.94	5.91
7	0.05	5.86	6.64	6.18

2.2.3. Database searches

The two common feature-based pharmacophores (hypo #2 and hypo #3) were used as search queries against the Catalyst™-formatted NCI2000 and Maybrdige2004 databases in order to retrieve molecules with novel chemical structures and desired chemical features. The Best Flexible Search/Spread Sheet method in Catalyst was used to search the databases. Hypo #2 retrieved 18 and 263 molecules from the NCI and Maybridge databases, respectively, while hypo #3 retrieved 38 and 328 molecules from the NCI and Maybridge databases, respectively.

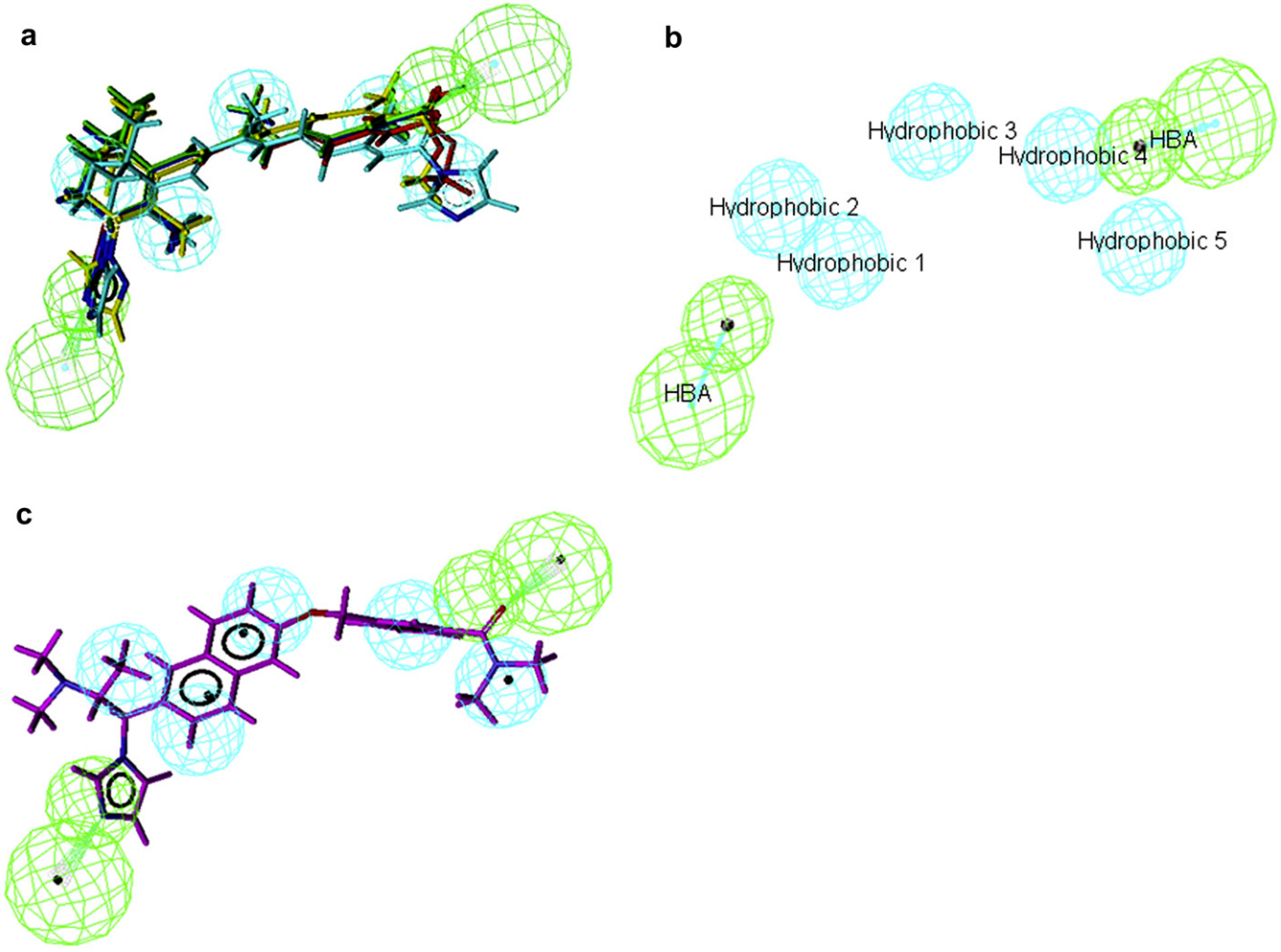

Fig. 4. Alignment of training set molecules with hypo 3 (**4a**), best hypo (hypo 3) selected on the basis of knowledge of ligand and enzyme interactions (**4b**) and alignment of hypo 3 with compound **2** (**4c**).

2.2.4. Biological activities of retrieved molecules from databases

We purchased some of the molecules obtained from the database searches (NCI and Maybridge) using these hypotheses. We selected molecules which were retrieved (a) by hypo #3 only, (b) by hypo #2 only, and (c) are common to both hypo #2 and hypo 3 with the hope that their activities would enable selection of the better hypothesis. These molecules (Chart 3) were tested for RAMBA activity in a hamster liver microsomal assay as previously described [43]. The biological activity testing results are reported as % inhibition and are shown in Table 6 and Fig. 5. Two compounds

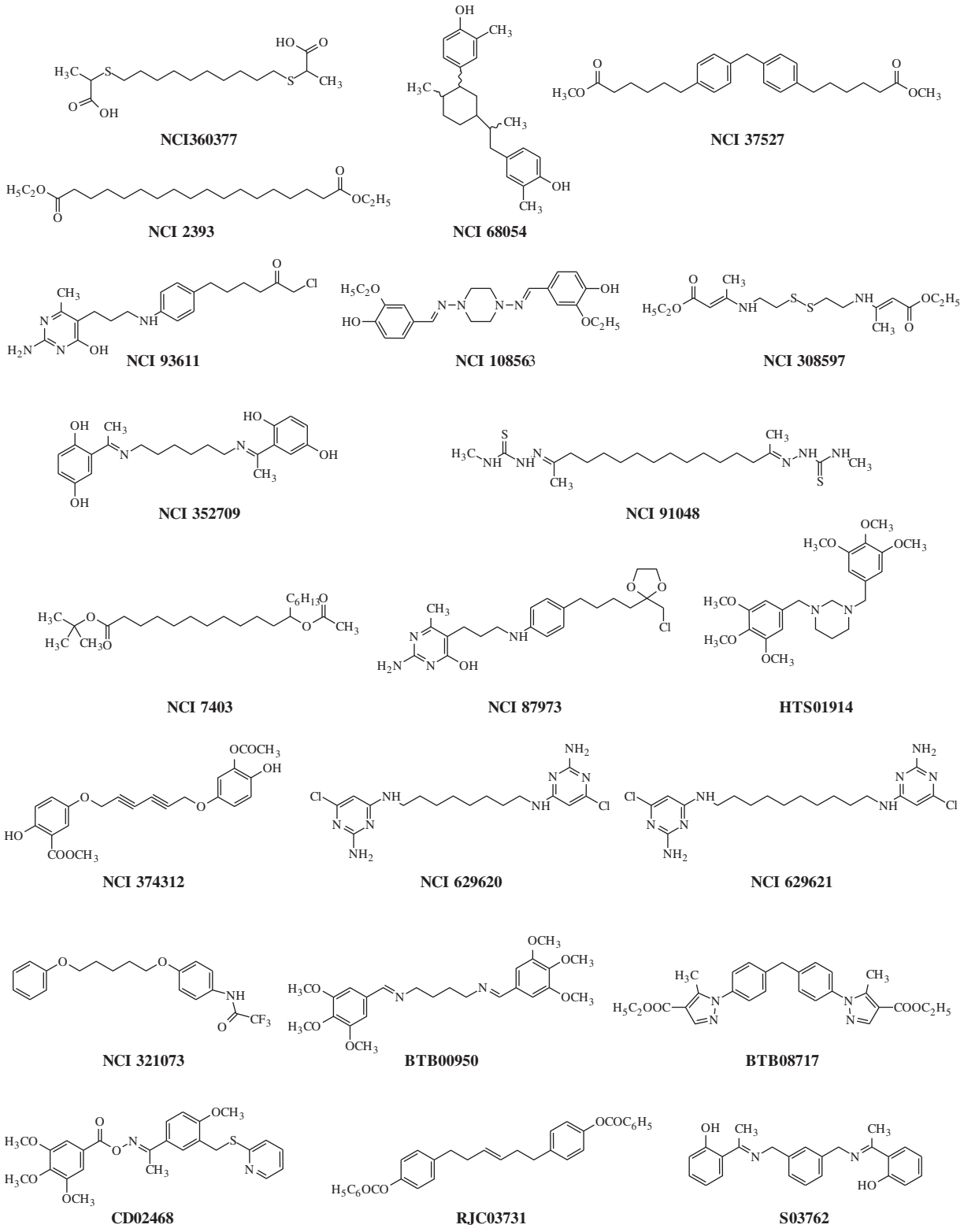

Chart 3. Structures of molecules retrieved from NCI and Maybridge databases.

Table 6
In vitro ATRA metabolism inhibitory activities of molecules obtained by database searching.

Sl. no.	Name	Fit		[a]Inhibition %
		Hypo 2	Hypo 3	
1	NCI360377	–	5.75	20.52
2	NCI68054	–	5.05	33.77
3	NCI37527	–	5.05	31.38
4	NCI2393	–	5.77	29.47
5	NCI0093611	–	5.3	42.78
6	NCI108563	–	5.19	34.27
7	NCI308597	–	5.15	54.73
8	NCI352709	–	5.17	22.186
9	NCI91048	–	5.06	21.22
10	NCI7403	–	5.46	36.168
11	NCI87973	–	5.64	29.36
12	HTS01914	–	5.36	53.24
13	NCI374312	–	5.46	17.94
14	NCI629620	4.92	–	18.07
15	NCI629621	5.06	–	32.70
16	NCI321073	4.27	–	34.785
17	BTB0950	1.27	5.21	27.317
18	BTB08717	4.10	4.92	49.785
19	CD02468	2.59	4.58	28.53
20	RJC03771	3.73	4.78	30.45
21	S03762	0.28	4.76	38.616

[a] Tested at 100 nM concentration of each compound by hamster liver microsome assay.

(NCI308597 and HTS01914) selected by hypo #3 showed >50% inhibition of ATRA metabolism by hamster liver microsomes, while one compound (BTB08717) selected by both hypos inhibited 49% of ATRA metabolism; none of the molecules selected by hypo #2 displayed ATRA metabolism inhibition more than 35%. NCI308597 and HTS01914 retrieved by hypo #3 showed higher activities than compounds retrieved by hypo #2. Molecules retrieved from database searching which are common to both hypos showed some activity, but the computed hypo-fit values were better correlated with hypo #3.

Based on all of these data, hypo #3 with five hydrophobic and two hydrogen bond acceptor features is chosen as a good representative computer-generated model for identifying new RAMBAs. The most active molecules in this study displayed less potency when compared to the training set molecules. The activity profile of these molecules correlate with the fit values computed from the hypothesis (<5.5 *vs.* 7 features). It is possible that searching of other commercial and/or proprietary databases may result in the identification of other potentially more active ATRA metabolism inhibitors.

2.3. Molecular modeling studies

To study the binding modes of the active hit molecules and our RAMBAs with the CYP26A enzyme, we performed molecular docking experiments of the following molecules ATRA, compounds **3**, **4**, NCI308597, and BTB08717 into the ligand binding site of the enzyme. ATRA was found to dock satisfactorily in the active site as previously reported [35,46]. The C-4 of cyclohexene ring positioned above the heme iron at the distance of 4.98 Å and the polyene chain passes through a hydrophobic tunnel made up of Phe84, Trp112, Phe119, Phe222, Pro371 and Phe374 to form hydrogen bonding interactions between carbonyl group of ATRA and Arg86. Similarly the retinoid RAMBAs (**3** and **4**) also form hydrogen bonding interactions with Arg86 and polyene chain covered with hydrophobic tunnel (Fig. 6). The imidazole group on C-4 of cyclohexene lies perpendicular to the heme iron at a distance of 4.22 Å. This distance would accommodate a water molecule between imidazole ring at

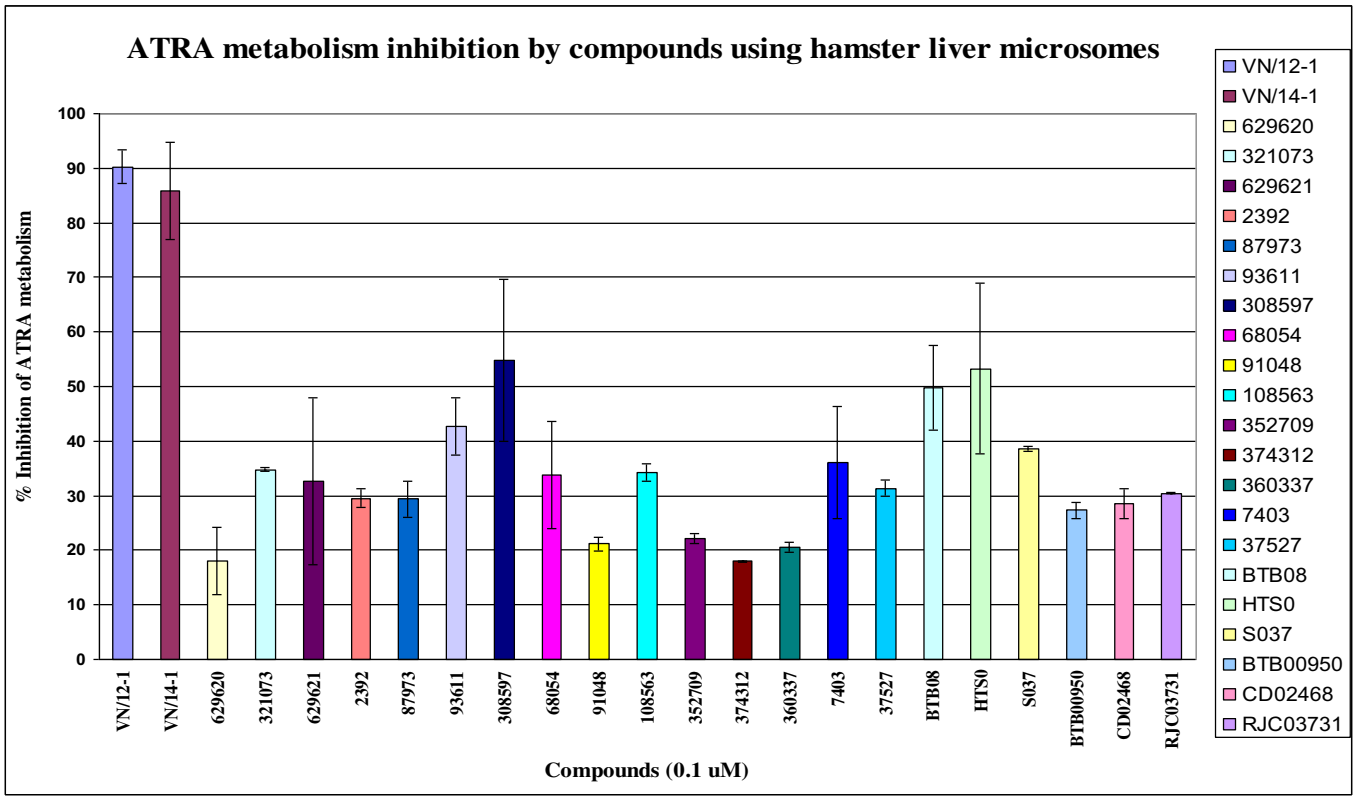

Fig. 5. ATRA metabolism inhibition by compounds using hamster liver microsomes.

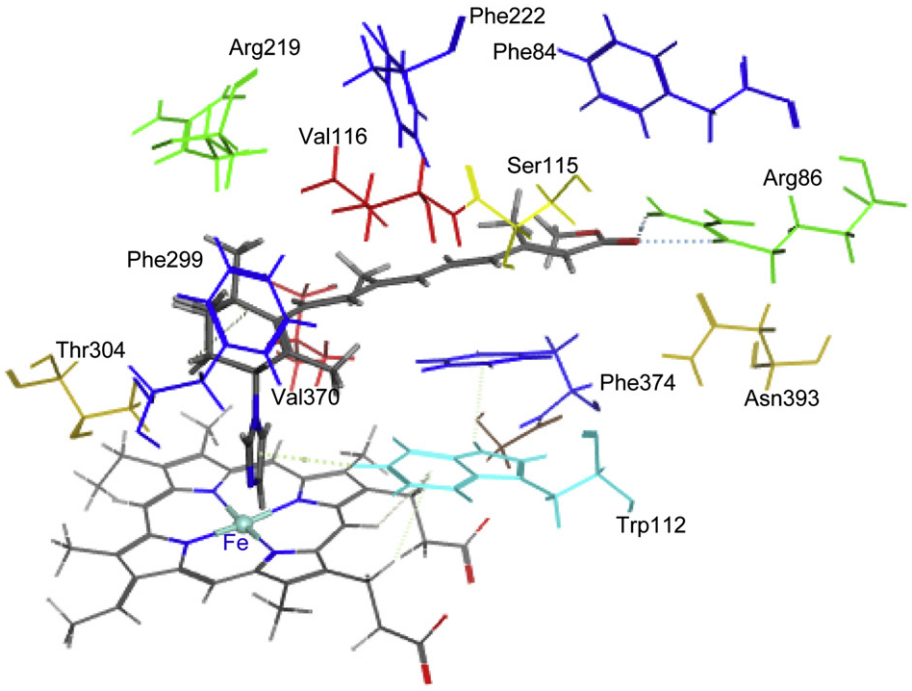

Fig. 6. Stereoview of the binding mode of compound **3** (color by element cap-stick) in the active site of CYP26A. The active site residues in the binding pocket are shown in different color (stick).

C-4 of compounds **3**, **4** and heme iron. In the case of NCI308597, one carbonyl group is oriented perpendicular to heme iron and the other carbonyl group at other end form hydrogen bonding interaction with Arg86. The scaffold holding two ester groups is surrounded by hydrophobic amino acids (Fig. 7). Similarly, two carbonyl groups at each end of BTB08717 are oriented toward the heme iron and Arg86 to form hydrophilic interactions (Fig. 8). The scaffold's diaryl ring is surrounded by hydrophobic amino acid residues. The interaction of ligands with active site is complimentary to pharmacophore model (hypo #3). Out of two hydrogen bond acceptors, one found around imidazole and triazole ring at C-4 position of cyclohexene is for interaction with heme iron and second one for interaction with Arg86. Five hydrophobic features are for interaction with hydrophobic tunnel formed by Phe84,

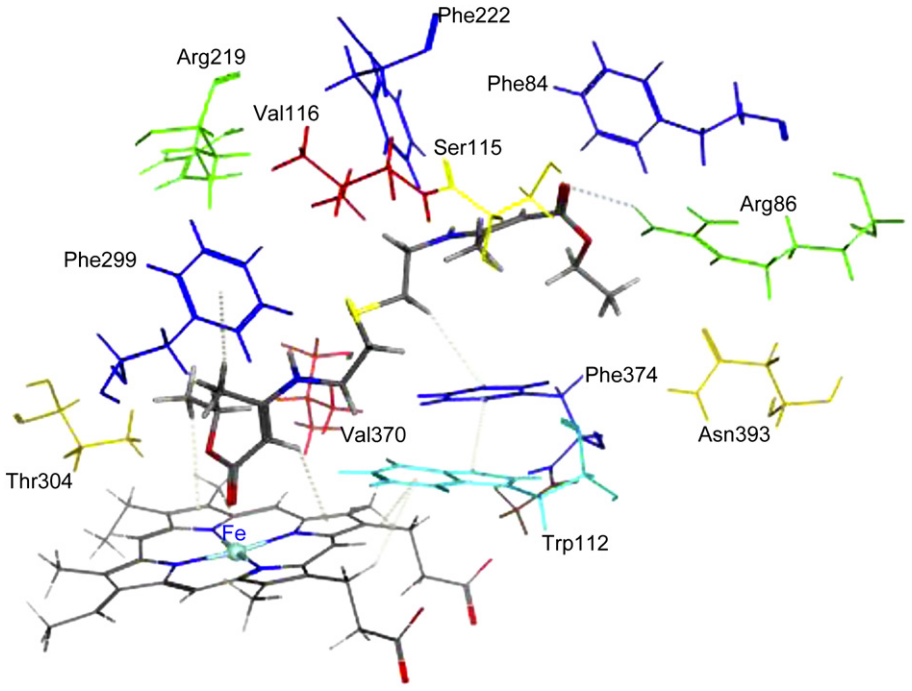

Fig. 7. Stereoview of the binding mode of NCI308597 (color by element with cap-stick) in the active site of CYP26A. The active site residues in the binding pocket are shown in different color (stick).

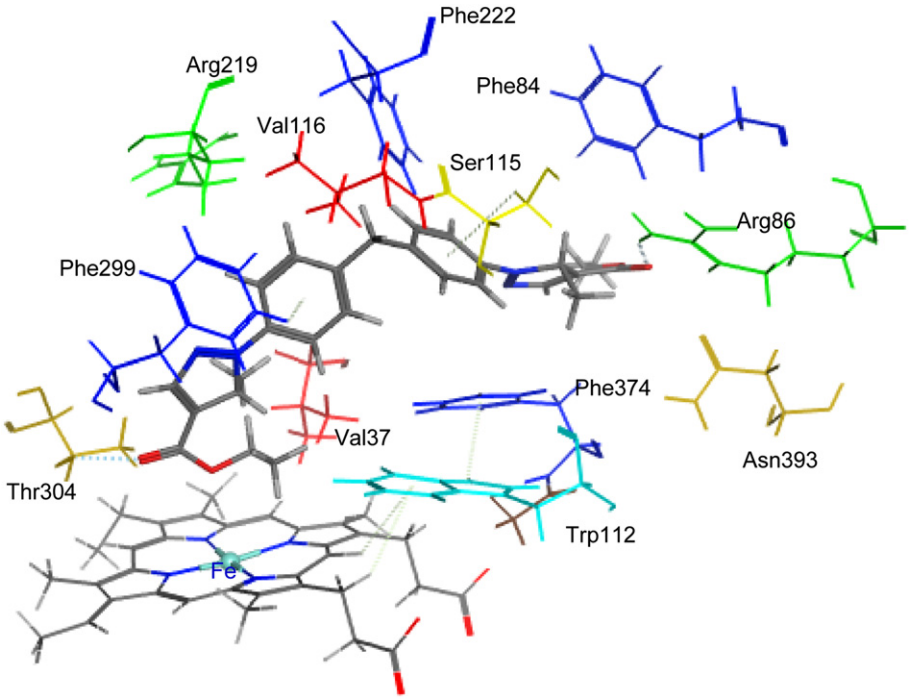

Fig. 8. Stereoview of the binding mode of BTB08717 (color by element with cap-stick) in the active site of CYP26A. The active site residues in the binding pocket are shown in different color (stick).

Trp112, Phe119, Phe222, Pro371 and Phe374 at active site. Clearly, these binding modes are similar to those reported for other known potent RAMBAs [35,36,46].

3. Conclusions

This chemical feature-based pharmacophore model and molecular docking study has provided the first insight into hypothetical ligand binding requirements for retinoic acid metabolism blocking agents. This hypothesis can be used for virtual screening of other databases to get insight for designing new and highly potent RAMBA inhibitors with possibly hitherto unknown scaffolds.

4. Experimental section

4.1. Chemistry

All the RAMBAs used in this study were synthesized in our laboratories and the methodologies for their preparation have been previously published [39,43]. The compounds identified by database searching were obtained from either the NCI (National Institute of Health, Bethesda, MD, USA) or Maybridge (Rayan Scientific, Inc., Isle of Palms. SC, USA).

4.2. In vitro assay of RAMBAs in hamster liver microsomal assay

We assessed ATRA hydroxylase activity in incubations containing liver or cancer cell microsomes and the inhibitors by measuring the radio-labeled polar metabolites produced from [11,12-^{3}H]-ATRA as we have previously described [43].

All enzymatic studies were performed in 0.1 M phosphate buffer, pH 7.4, at a final incubation volume of 0.40 mL. The incubation mixture contained 100 μL of microsomes (500 μg/mL dissolved in buffer); 100 μL of NADPH (20 mM dissolved in dH_2O); 40 μL of inhibitor (dissolved in DMSO); and 140 μL of assay buffer [0.01 M $MgCl_2$ and 0.02 (w/v) bovine serum albumin (BSA) in phosphate buffer solution]. After a 3-min preincubation at 37 °C, the reaction was initiated by the addition of 20 μM of [11,12-^{3}H]-ATRA (20 μCi/mL) and the incubation was carried out for 30 min under oxygen with shaking in a water bath at 37 °C. The reaction was terminated by the addition of 100 μL of formic acid. The retinoid products were extracted (2×) with 1 mL of ethyl acetate containing 10% methanol and 0.05% butylated hydroxyanisole (BHA). The organic and aqueous phases are separated by centrifugation at 3000 g for 10 min at 4 °C. The organic phase, containing the retinoids, was dried with a stream of argon and dissolved in 100 μL of methanol for HPLC analysis.

4.3. Generation of pharmacophore models

Pharmacophore modeling studies was performed using Catalyst 4.10 [47] installed on Silicon Graphics O_2 desktop work-station equipped with a 300 MHz MIPS R5000 processor (128 MB RAM) running the Irix 6.5 operating system.

All structures were generated using 2D/3D editor sketcher and minimized to the closest minimum using the CHARMm-like force field implemented in the program [60]. Regarding the asymmetric centers of all the compounds, as no experimental data on the biologically relevant conformations of these molecules is available; it was arbitrarily decided to assign 'undefined' chirality. Allowing the pharmacophore model to choose which configuration of the asymmetric carbon atoms is the most appropriate. A stochastic research coupled to a poling method [61] was applied to generate conformers for each compound by using 'Best conformer generation' option with 20 kcal/mol energy cutoff (20 kcal/mol maximum compared to the most stable conformer).

The pharmacophore-based investigation of RAMBAs involved using the catalyst/HipHop program to generate feature-based 3D pharmacophore alignments [62,63]. This was performed in a three-step procedure [64]: (a) a conformation model for each molecule in the training set was generated; (b) each conformer was examined for the presence of chemical feature; (c) a three-dimensional

configuration of chemical feature common to the input molecules was determined. Catalyst provides a dictionary of chemical features found to be important in drug-enzyme/receptor interactions. These are hydrogen bond donors, hydrogen bond acceptors, hydrophobic groups, ring aromatic and positive and negative ionizable groups. For the pharmacophore modeling runs, common features selected for the run were ring aromatic (R), hydrogen bond donor (D), hydrogen bond acceptor (A), and hydrophobic group (H).

4.4. Molecular docking

All molecular modeling calculations related to docking studies were performed using 'Molecular Operating Environment (MOE) version 2010.10 release of Chemical Computing Group's [65], on a Windows Vista operating system installed on an Intel® Core™2 Duo 2.2 GHz processor and 3 GB RAM. The target compounds were built using the MOE builder interface and subjected to energy minimization using MMFF94x force field and the partial charges were computed using the same force field. Homology model of human retinoic acid metabolizing enzyme Cytochrome P450 26A1 (CYP26A1) was used for docking was provided by Drs. C. Simons and Andrea Brancale. The enzyme was prepared for the docking studies where: (i) hydrogen atoms were added to the structure with their standard geometry; (ii) heme was defined as part of receptor; (iii) partial charges were computed using Amber99 force field. The active site was defined by all the amino acid residues within a 6.5 Å distance from ligand atom. Docking calculations were done using Alpha triangle placement method and poses were prioritized by London dG scoring method.

Acknowledgement

This research was supported by grants from US National Institutes of Health and National Cancer Institute (R21 CA117991-01, 1R01CA129379-01 A2 and 5R01CA129379-02) to Professor Vincent C. O. Njar. We also thank Dr. Claire Simons, Welsh School of Pharmacy, Cardiff University, Cardiff, UK for providing CYP26A enzyme homology model used for docking studies.

References

[1] M.B. Sporn, Carcinogenesis and cancer: different perspectives on the same disease, Cancer Res. 51 (1991) 6215–6218.
[2] R.P. Warrell, in: V.T. DeVita, S. Hellman, S.A. Rosenberg (Eds.), Cancer, Principles & Practice of Oncology, J.B. Lippincott, Philadelphia, PA, 1977, pp. 483–490.
[3] R. Lotan, Retinoids in cancer chemoprevention, FASEB J. 10 (1996) 1031–1039.
[4] R.C. Moon, R.G. Mehta, K.V.N. Rao, Retinoids and cancer in experimental animals. in: M.B. Sporn, A.B. Roberts, D.S. Goodman (Eds.), The Retinoids: Biology, Chemistry, and Medicine. Raven Press Ltd., New York, NY, 1994, pp. 573–595.
[5] M.B. Sporn, N.M. Dunlop, D.L. Newton, J.M. Smith, Prevention of chemical carcinogenesis by vitamin A and its synthetic analogs (retinoids), Fed. Proc. 35 (1976) 1332–1338.
[6] M.A. Smith, D.R. Parkinson, B.D. Cheson, M.A. Friedman, Retinoids in cancer therapy, J. Clin. Oncol. 10 (1992) 839–864.
[7] M.B. Sporn, A.B. Roberts, S.G. DeWitt, The Retinoids: Biology, Chemistry and Medicine. Raven Press, New York, 1994.
[8] S.K. Patra, A. Patra, R. Dahiya, Histone deacetylase and DNA methyltransferase in human prostate cancer, Biochem. Biophys. Res. Commun. 287 (2001) 705–713.
[9] D.J. Mangelsdorf, K. Umesono, R.M. Evans, in: M.B. Sporn, A.B. Roberts, D.S. Goodman (Eds.), The Retinoids: Biology, Chemistry, and Medicine, Raven, New York, 1994, pp. 319–349.
[10] J. Muindi, S.R. Frankel, W.H. Miller Jr., A. Jakubowski, D.A. Scheinberg, C.W. Young, E. Dmitrovsky, R.P. Warrell Jr., Continuous treatment with all-trans retinoic acid causes a progressive reduction in plasma drug concentrations: implications for relapse and retinoid "resistance" in patients with acute promyelocytic leukemia, Blood 79 (1992) 299–303.
[11] J.F. Muindi, H.I. Scher, J.R. Rigas, R.P. Warrell Jr., C.W. Young, Elevated plasma lipid peroxide content correlates with rapid plasma clearance of all-*trans*-retinoic acid in patients with advanced cancer, Cancer Res. 54 (1994) 2125–2128.
[12] J.S. Lee, R.A. Newman, S.M. Lippman, M.H. Huber, T. Minor, M.N. Raber, I.H. Krakoff, W.K. Hong, Phase I evaluation of all-*trans*-retinoic acid in adults with solid tumors, J. Clin. Oncol. 11 (1993) 959–966.
[13] W.H. Miller Jr., The emerging role of retinoids and retinoic acid metabolism blocking agents in the treatment of cancer, Cancer 83 (1998) 1471–1482.
[14] V.C. Njar, Cytochrome p450 retinoic acid 4-hydroxylase inhibitors: potential agents for cancer therapy, Mini-Rev. Med. Chem. 2 (2002) 261–269.
[15] E. Freyne, A. Raeymaekers, M. Venet, G. Sanz, W. Wouters, R. De Coster, J.V. Wauwe, Synthesis of LIAZAL, a retinoic acid metabolism blocking agent (RAMBA) with potential clinical applications in oncology and dermatology, Bioorg. Med. Chem. Lett. 8 (1998) 267–272.
[16] S.M. Thacher, J. Vasudevan, K.Y. Tsang, S. Nagpal, R.A. Chandraratna, New dermatological agents for the treatment of psoriasis, J. Med. Chem. 44 (2001) 281–297.
[17] C.A. Frolik, A.B. Roberts, T.E. Tavela, P.P. Roller, D.L. Newton, M.B. Sporn, Isolation and identification of 4-hydroxy- and 4-oxoretinoic acid. In vitro metabolites of all-*trans*-retinoic acid in hamster trachea and liver, Biochemistry 18 (1979) 2092–2097.
[18] L.C. McSorley, A.K. Daly, Identification of human cytochrome P450 isoforms that contribute to all-trans-retinoic acid 4-hydroxylation, Biochem. Pharmacol. 60 (2000) 517–526.
[19] L. Nadin, M. Murray, Participation of CYP2C8 in retinoic acid 4-hydroxylation in human hepatic microsomes, Biochem. Pharmacol. 58 (1999) 1201–1208.
[20] J. Marill, T. Cresteil, M. Lanotte, G.G. Chabot, Identification of human cytochrome P450s involved in the formation of all-trans-retinoic acid principal metabolites, Mol. Pharmacol. 58 (2000) 1341–1348.
[21] S.S. Abu-Abed, B.R. Beckett, H. Chiba, J.V. Chithalen, G. Jones, D. Metzger, P. Chambon, M. Petkovich, Mouse P450RAI (CYP26) expression and retinoic acid-inducible retinoic acid metabolism in F9 cells are regulated by retinoic acid receptor gamma and retinoid X receptor alpha, J. Biol. Chem. 273 (1998) 2409–2415.
[22] W.J. Ray, G. Bain, M. Yao, D.I. Gottlieb, CYP26, a novel mammalian cytochrome P450, is induced by retinoic acid and defines a new family, J. Biol. Chem. 272 (1997) 18702–18708.
[23] E. Sonneveld, P.T. van der Saag, Metabolism of retinoic acid: implications for development and cancer, Int. J. Vitam. Nutr. Res. 68 (1998) 404–410.
[24] J.A. White, B. Beckett-Jones, Y.D. Guo, F.J. Dilworth, J. Bonasoro, G. Jones, M. Petkovich, cDNA cloning of human retinoic acid-metabolizing enzyme (hP450RAI) identifies a novel family of cytochromes P450, J. Biol. Chem. 272 (1997) 18538–18541.
[25] J.A. White, Y.D. Guo, K. Baetz, B. Beckett-Jones, J. Bonasoro, K.E. Hsu, F.J. Dilworth, G. Jones, M. Petkovich, Identification of the retinoic acid-inducible all-trans-retinoic acid 4-hydroxylase, J. Biol. Chem. 271 (1996) 29922–29927.
[26] J. Marill, N. Idres, C.C. Capron, E. Nguyen, G.G. Chabot, Retinoic acid metabolism and mechanism of action: a review, Curr. Drug. Metab. 4 (2003) 1–10.
[27] P.V. Bhat, A. Lacroix, Metabolism of retinol and retinoic acid in N-methyl-N-nitrosourea-induced mammary carcinomas in rats, Cancer Res. 49 (1989) 139–144.
[28] I.S. Han, J.H. Choi, Highly specific cytochrome P450-like enzymes for all-trans-retinoic acid in T47D human breast cancer cells, J. Clin. Endocrinol. Metab. 81 (1996) 2069–2075.
[29] M.D. Krekels, A. Verhoeven, J. van Dun, W. Cools, C. Van Hove, L. Dillen, M.C. Coene, W. Wouters, Induction of the oxidative catabolism of retinoid acid in MCF-7 cells, Br. J. Cancer 75 (1997) 1098–1104.
[30] M.D. Krekels, J. Zimmerman, B. Janssens, R. Van Ginckel, W. Cools, C. Van Hove, M.C. Coene, W. Wouters, Analysis of the oxidative catabolism of retinoic acid in rat Dunning R3327G prostate tumors, Prostate 29 (1996) 36–41.
[31] E. Sonneveld, C.E. van den Brink, B.M. van der Leede, R.K. Schulkes, M. Petkovich, B. van der Burg, P.T. van der Saag, Human retinoic acid (RA) 4-hydroxylase (CYP26) is highly specific for all-trans-RA and can be induced through RA receptors in human breast and colon carcinoma cells, Cell Growth Differ. 9 (1998) 629–637.
[32] B.M. van der Leede, C.E. van den Brink, W.W. Pijnappel, E. Sonneveld, P.T. van der Saag, B. van der Burg, Autoinduction of retinoic acid metabolism to polar derivatives with decreased biological activity in retinoic acid-sensitive, but not in retinoic acid-resistant human breast cancer cells, J. Biol. Chem. 272 (1997) 17921–17928.
[33] J.V.G. Van Heusden, R. Bruwiere, H. Moelans, P. Janssen, B. Floren, W. van der Leede, B.J. van Dun, G. Sanz, M. Venet, L. Dillen, C. Van Hove, G. Willemsens, M. Janicot, W. Wouters, Inhibition of all-TRANS-retinoic acid metabolism by R116010 induces antitumour activity, Br. J. Cancer 86 (2002) 605–611.
[34] W. Wouters, J. van Dun, A. Dillen, M.C. Coene, W. Cools, R. De Coster, Effects of liarozole, a new antitumoral compound, on retinoic acid-induced inhibition of cell growth and on retinoic acid metabolism in MCF-7 human breast cancer cells, Cancer Res. 52 (1992) 2841–2846.
[35] M.S. Gomaa, J.L. Armstrong, B. Bobillon, G.J. Veal, A. Brancale, C.P. Redfern, C. Simons, Novel azolyl-(phenylmethyl)]aryl/heteroarylamines: potent CYP26 inhibitors and enhancers of all-trans retinoic acid activity in neuroblastoma cells, Bioorg. Med. Chem. 16 (2008) 8301–8313.
[36] M.S. Gomaa, C.E. Bridgens, A.S. Aboraia, G.J. Veal, C.P. Redfern, A. Brancale, J.L. Armstrong, C. Simons, Small molecule inhibitors of retinoic acid 4-hydroxylase (CYP26): synthesis and biological evaluation of imidazole

methyl 3-(4-(aryl-2-ylamino)phenyl)propanoates, J. Med. Chem. 54 (2011) 2778–2791.
[37] P. McCaffery, C. Simons, Prospective teratology of retinoic acid metabolic blocking agents (RAMBAs) and loss of CYP26 activity, Curr. Pharm. Des. 13 (2007) 3020–3037.
[38] V.C. Njar, L. Gediya, P. Purushottamachar, P. Chopra, T.S. Vasaitis, A. Khandelwal, J. Mehta, C. Huynh, A. Belosay, J. Patel, Retinoic acid metabolism blocking agents (RAMBAs) for treatment of cancer and dermatological diseases, Bioorg. Med. Chem. 14 (2006) 4323–4340.
[39] V.C. Njar, I.P. Nnane, A.M. Brodie, Potent inhibition of retinoic acid metabolism enzyme(s) by novel azolyl retinoids, Bioorg. Med. Chem. Lett. 10 (2000) 1905–1908.
[40] R.D. Bruno, V.C. Njar, Targeting cytochrome P450 enzymes: a new approach in anti-cancer drug development, Bioorg. Med. Chem. 15 (2007) 5047–5060.
[41] L.K. Gediya, A. Belosay, A. Khandelwal, P. Purushottamachar, V.C. Njar, Improved synthesis of histone deacetylase inhibitors (HDIs) (MS-275 and CI-994) and inhibitory effects of HDIs alone or in combination with RAMBAs or retinoids on growth of human LNCaP prostate cancer cells and tumor xenografts, Bioorg. Med. Chem. 16 (2008) 3352–3360.
[42] L.K. Gediya, A. Khandelwal, J. Patel, A. Belosay, G. Sabnis, J. Mehta, P. Purushottamachar, V.C. Njar, Design, synthesis, and evaluation of novel mutual prodrugs (hybrid drugs) of all-trans-retinoic acid and histone deacetylase inhibitors with enhanced anticancer activities in breast and prostate cancer cells in vitro, J. Med. Chem. 51 (2008) 3895–3904.
[43] J.B. Patel, C.K. Huynh, V.D. Handratta, L.K. Gediya, A.M. Brodie, O.G. Goloubeva, O.O. Clement, I.P. Nanne, D.R. Soprano, V.C. Njar, Novel retinoic acid metabolism blocking agents endowed with multiple biological activities are efficient growth inhibitors of human breast and prostate cancer cells in vitro and a human breast tumor xenograft in nude mice, J. Med. Chem. 47 (2004) 6716–6729.
[44] J.B. Patel, A. Khandelwal, P. Chopra, V.D. Handratta, V.C. Njar, Murine toxicology and pharmacokinetics of novel retinoic acid metabolism blocking agents, Cancer Chemother. Pharmacol. 60 (2007) 899–905.
[45] J.B. Patel, J. Mehta, A. Belosay, G. Sabnis, A. Khandelwal, A.M. Brodie, D.R. Soprano, V.C. Njar, Novel retinoic acid metabolism blocking agents have potent inhibitory activities on human breast cancer cells and tumour growth, Br. J. Cancer 96 (2007) 1204–1215.
[46] M.S. Gomaa, S.W. Yee, C.E. Milbourne, M.C. Barbera, C. Simons, A. Brancale, Homology model of human retinoic acid metabolising enzyme cytochrome P450 26A1 (CYP26A1): active site architecture and ligand binding, J. Enzyme Inhib. Med. Chem. 21 (2006) 361–369.
[47] Catalyst, Release Version 4.10, Accelrys, 9685 Scranton Road, San Diego, CA 92121.
[48] O.O. Clement, C.M. Freeman, R.W. Hartmann, V.D. Handratta, T.S. Vasaitis, A.M. Brodie, V.C. Njar, Three dimensional pharmacophore modeling of human CYP17 inhibitors. Potential agents for prostate cancer therapy, J. Med. Chem. 46 (2003) 2345–2351.
[49] P. Purushottamachar, A. Khandelwal, P. Chopra, N. Maheshwari, L.K. Gediya, T.S. Vasaitis, R.D. Bruno, O.O. Clement, V.C.O. Njar, First pharmacophore-based identification of androgen receptor down-regulating agents: discovery of potent anti-prostate cancer agents, Bioorg. Med. Chem. 15 (2007) 3413–3421.
[50] M.L. Lopez-Rodriguez, B. Benhamu, T. de la Fuente, A. Sanz, L. Pardo, M. Campillo, A three-dimensional pharmacophore model for 5-hydroxytryptamine6 (5-HT6) receptor antagonists, J. Med. Chem. 48 (2005) 4216–4219.
[51] J.X. Ren, L.L. Li, J. Zou, L. Yang, J.L. Yang, S.Y. Yang, Pharmacophore modeling and virtual screening for the discovery of new transforming growth factor-beta type I receptor (ALK5) inhibitors, Eur. J. Med. Chem. 44 (2009) 4259–4265.
[52] B. Waltenberger, K. Wiechmann, J. Bauer, P. Markt, S.M. Noha, G. Wolber, J.M. Rollinger, O. Werz, D. Scuster, S. Hermann, Pharmacophore modeling and virtual screening of novel acidic inhibitors of microsomal prostaglandin E_2 synthase-1 (mPGES-1), J. Med. Chem. 54 (2011) 3163–3174.
[53] Z. Wang, S. Zhang, H. Jin, W. Wang, J. Huo, L. Zhou, Y. Wang, F. Feng, L. Zhang, Angiotensin-1-converting enzyme inhibitory peptides: chemical feature based pharmacophore generation, Eur. J. Med. Chem. 46 (2011) 3428–3433.
[54] D. Barnum, J. Greene, A. Smellie, P. Sprague, Identification of common functional configurations among molecules, J. Chem. Inf. Comput. Sci. 36 (1996) 563–571.
[55] L.H. Sutte, R. Hoffmann, Hypogen: an automated system for generating 3D predictive pharmacophore models. in: O.F. Guner (Ed.), IPharmacophore Perception, Development, and Use in Drug Design. International University Line, La Jolla, CA, 2000, pp. 171–189.
[56] O.F. Güner, Metric for analyzing hit lists and pharmacophores. in: O.F. Güner (Ed.), Pharmacophore Perception, Development, and Use in Drug Design. International University Line, La Jolla, CA, 2000, pp. 191–211.
[57] O.F. Guner, Strategies for database mining and pharmacophore development. in: O.F. Guner (Ed.), Pharmacophore Perception, development, and Use in Drug Design. International University Line, La Jolla, CA, 2000, pp. 213–236.
[58] E.S. Edger, J.D. Holliday, P.L. Willett, J. Mol. Graphics Modell. 18 (2000) 343–375.
[59] M.J. Mulvihill, J.L. Kan, P. Beck, M. Bittner, C. Cesario, A. Cooke, D.M. Keane, A.I. Nigro, C. Nillson, V. Smith, M. Srebernak, F.L. Sun, M. Vrkljan, S.L. Winski, A.L. Castelhano, D. Emerson, N. Gibson, Potent and selective [2-imidazol-1-yl-2-(6-alkoxy-naphthalen-2-yl)-1-methyl-ethyl]-dimethylamines as retinoic acid metabolic blocking agents (RAMBAs), Bioorg. Med. Chem. Lett. 15 (2005) 1669–1673.
[60] R.B. Brooks, R.E. Bruccoleri, B.D. Olafson, D.J. States, S. Swaminathan, M. Karplus, Charmm – a program for macromolecular energy, minimization, and dynamics calculations, J. Comp. Chem. 4 (1983) 187–217.
[61] A. Smellie, S.L. Teig, P. Towbin, Poling: promoting conformational variation, J. Comput. Chem. 16 (1995) 171–187.
[62] J. Greene, S. Kahn, H. Savoj, P. Sprague, S. Teig, Chemical function queries for 3D database search, J. Chem. Inf. Comput. Sci. 34 (1994) 1297–1308.
[63] P.W. Sprague, Automated chemical hypotheses generation and database searching with catalyst. in: K. Müller (Ed.), Perspectives in Drug Discovery and Design. ESCOM Science Publishers, Leiden, B.V., The Netherlands, 1995, pp. 1–20.
[64] O.O. Clement, A. Trope-Mehl, HipHop: pharmacophores based on multiple common-feature alignments. in: O.F. Güner (Ed.), Pharmacophore Perception, Development, and Use in Drug Design. International University Line, La Jolla, CA, 2000, pp. 69–83.
[65] M.O.E. (MOE). Chemical Computing Group, Inc, Montreal, Quebec, Canada, 2010.